JOURNAL OF CATALYSIS 93, 417–429 (1985)

Solid-Electrolyte-Aided Study of Hydrogen Oxidation on Nickel

CONSTANTINO SARANTEAS AND MICHAEL STOUKIDES

Department of Chemical Engineering, Tufts University, Medford, Massachusetts 02155

Received June 21, 1984; revised January 15, 1985

The catalytic oxidation of hydrogen on porous polycrystalline Ni films supported on stabilized zirconia was studied at temperatures between 240 and 410°C and atmospheric total pressure. The technique of solid electrolyte potentiometry (SEP) was used to monitor the chemical potential of oxygen adsorbed on the nickel catalyst. The steady-state kinetic and potentiometric measurements indicate formation of a stable nickel oxide and its reduction by hydrogen. Over a wide range of temperature and gas composition both the reaction rate and the surface oxygen activity exhibit sustained oscillatory behavior. A kinetic model based on the kinetic and potentiometric results is discussed.

INTRODUCTION

The catalytic oxidation of hydrogen has attracted considerable attention in recent years because (a) in spite of its simplicity and technical interest there have been surprisingly few fundamental studies of the oxidation of hydrogen and the kinetics is not well established even for the metals that are most active (*1*) and (b) it has been reported that under certain conditions the catalytic oxidation of H_2 on Pt, Pd, and Ni exhibits sustained oscillatory behavior, a phenomenon of both theoretical and practical importance (*2, 3*).

As early as 1924 Larson and Smith studied the nickel-catalyzed hydrogen oxidation at 34–130°C and at oxygen concentrations of up to 2% (*4*). Larson and Smith suggested that at least two reactions take place, each reaction involving the formation of an oxide and its subsequent reduction by hydrogen. Later Gidaspow and Ellington (*5*) studied the rate behavior of the oxidation of H_2 in excess air and Mamedov *et al.* (*6*) examined the effect of the chemical nature of the catalyst on the reaction rate.

Since 1973 a number of investigators have reported oscillatory behavior during the oxidation of H_2 on Ni (*7–13*). Belyaev *et al.* showed that oscillations started developing at some critical O_2 concentration with the amplitude increasing, reaching a maximum and then diminishing with increasing O_2 concentration (*7–9*). Schmitz *et al.* (*10*) studied the above reaction on a nickel foil under nonisothermal conditions and observed that oscillatory states develop for oxygen concentrations between 1 and 5% while stable nonoscillatory states were found over the entire region of O_2 concentrations examined, i.e., 0 to 7%. One of the most interesting features examined by Schmitz *et al.* was the hysteresis phenomenon which was also reported by Kurtanjek *et al.* (*11*). Kurtanjek *et al.* studied the reaction behavior in conjunction with Contact Potential Difference measurements (CPD) which enabled them to relate the oscillatory phenomena to changes in the work function of the catalyst surface. The above author has recently proposed a mathematical model based on assumption of simultaneous oxidation and reduction of the surface (*14*). Sault and Masel studied the effect of surface protrusions on thermal oscillations during H_2 oxidation on a Ni foil (*13*). The above investigators observed absence of sustained oscillations when using highly polished catalysts and development of self-sustained oscillations when the catalysts

0021-9517/85 $3.00

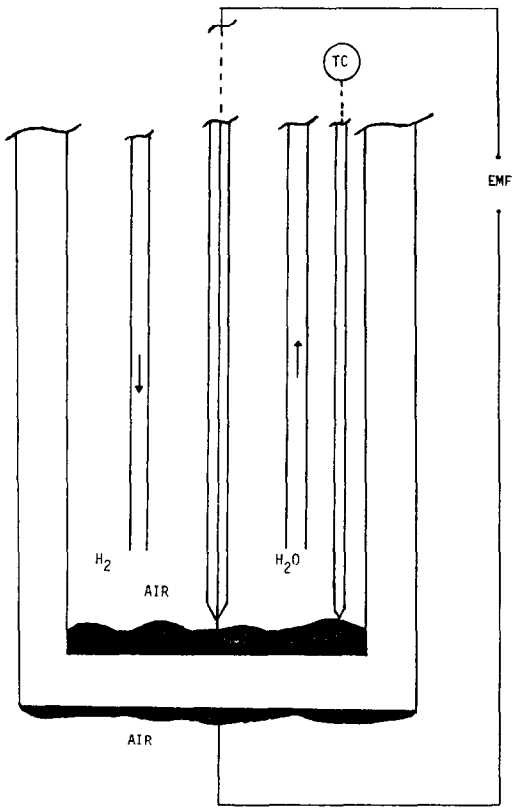

FIG. 1. Reactor cell configuration.

were used without the appropriate pretreatment.

In the present study the oxidation of H_2 was studied on a polycrystalline Ni film over a wide range of temperature and gas composition. The technique of Solid Electrolyte Potentiometry (SEP) was used in order to monitor the thermodynamic activity of oxygen adsorbed on the catalyst surface. To this end the nickel film was supported on stabilized zirconia, a pure-oxygen ion conductor. The above technique originally proposed by Wagner (*15*) provides a continuous and *in situ* measurement of the activity of adsorbed oxygen and has been used so far in a number of kinetic studies (*16–18*). Particular emphasis is given in this study in the stable nonoscillatory behavior of the catalyst. The recent studies (*7–13*) of the above reaction have provided detailed information on the dynamic behavior of the system and specifically on the development of oscillatory and chaotic phenomena in the reaction rate. Nevertheless, the isothermal stable steady-state kinetics has not been well investigated. It is clear that a model attempting to explain the periodic phenomena should satisfy the stable steady-state kinetics as well.

Various theoretical models have been developed in order to explain periodic phenomena observed in catalytic reactions (*19–24*). There still exists, however, a gap between experimental observations and theoretical mechanisms proposed. Thus knowledge of the reaction kinetics in the stable steady-state regime can serve as a useful tool for discriminating among rival kinetic models and assumptions.

EXPERIMENTAL METHODS

Apparatus. The experimental apparatus consisted of the flow system, the reactor cell, and the analytical system. Details on the flow system and the reactor cell can be found elsewhere (*25, 26*). The reactor cell configuration is shown in Fig. 1. It was a 30.3-cm^3-volume stabilized zirconia tube with an internal cross section of 2 cm^2, identical to those used in previous SEP studies (*16–18*). The nickel catalyst film was deposited on the flat bottom of the tube. Under the flow rates employed in this study the reactor has been shown (*25*) to behave like a CSTR. A stainless-steel cap was clamped to the open end of the tube. The cap provided for introduction and removal of gases, introduction of a Ni wire enclosed in a Pyrex tube to establish contact with the inside catalyst electrode, as well as for introduction of a thermocouple attached to the catalyst film (Fig. 1). The cap was cooled. The reactor was located in a furnace where the temperature was controlled within 1°C by means of an Omega Model 49K temperature controller. AIRCO ultrahigh-purity hydrogen and air were used as the reactant gases, while prepurified nitrogen was used as a diluent. The oxygen concentration in the feed or the efflu-

ent stream was measured continuously by means of a Beckman 755 paramagnetic oxygen analyzer. A J. Fluke 8600A voltmeter was used for the SEP measurements. The voltmeter and the oxygen analyzer readings were recorded on a two-pen chart recorder.

Measurement of surface oxygen activity. Solid electrolyte potentiometry (SEP) was used to measure *in situ* the thermodynamic activity of oxygen on the nickel catalyst film. It has been well established (*15, 25*) that the measured open-circuit emf reflects the difference in chemical potential of oxygen adsorbed on the two electrodes (Fig. 1):

$$E = \frac{1}{4F}\left[\mu_{O_2}\,(\text{catalyst}) - \mu_{O_2}\,(\text{reference})\right]. \quad (1)$$

The chemical potential of oxygen adsorbed on the reference electrode which is in contact with air ($P_{O_2} \simeq 0.21$ bar) is given by

$$\mu_{O_2}\,(\text{reference}) = \mu^{\circ}_{O_2}\,(\text{g}) + RT \ln(0.21), \quad (2)$$

where $\mu^{\circ}_{O_2}$ (g) is the standard chemical potential of oxygen at the temperature of interest. The activity a_0 of adsorbed atomic oxygen is defined by the equation

$$\mu_{O_2}\,(\text{catalyst}) = \mu^{\circ}_{O_2}\,(\text{g}) + RT \ln a_0^2. \quad (3)$$

Thus a_0^2 expresses the partial pressure of gaseous oxygen that would be in thermodynamic equilibrium with oxygen adsorbed on the nickel surface, if such an equilibrium were established. Therefore combining Eqs. (1), (2), and (3) a_0 is given by

$$a_0 = (0.21)^{1/2} \exp\left(\frac{2FE}{RT}\right). \quad (4)$$

The above equation is always valid irrespective of whether thermodynamic equilibrium is established between adsorbed and gas phase oxygen or not. In the special case that thermodynamic equilibrium indeed exists between gaseous and adsorbed oxygen, then

$$a_0^2 = P_{O_2}. \quad (5)$$

In the present study the nickel catalyst served as the inside electrode (Fig. 1). On the outside wall a silver film instead of a nickel film was deposited mainly because silver adheres to the zirconia wall much stronger than nickel. This caused a slight (2–6 mV) change in the reference measurements and was appropriately taken into account in the oxygen activity calculations (*26*).

The basic difference between SEP and CPD used by Luss *et al.* (*11*) is that CPD measures changes in the work function of the metal resulting from all adsorbed species (oxygen, hydrogen, etc.) while SEP measures specifically changes in the chemical potential of adsorbed oxygen only.

Catalyst preparation and characterization. The Ni catalyst film was prepared using Englehard No. 58-A nickel resinate. A few drops of the resinate solution were applied to the zirconia surface followed by drying and heating at 400°C for 2 h. The catalyst was then subjected to several cycles of oxidation and reduction. During each cycle the catalyst was exposed to a hydrogen stream for 12 h followed by oxidation in an oxygen stream for 2 h. The surface was assumed to be clean after reproducible voltage readings were obtained in successive reduction–oxidation cycles. Following the procedure adopted by Kurtanjek *et al.* (*11*) the catalyst was heated to 400°C and reduced in a hydrogen stream for 10 h after the end of each experiment. The above pretreatment method gave reproducible results over a period of several weeks. The loss of catalyst activity over that period was insignificant.

The outside silver electrode was prepared from silver suspension in butyl acetate. The silver electrode preparation has been described in detail elsewhere (*25*).

The surface of the Ni catalyst was examined using Scanning Electron Microscopy (SEM). Figure 2 shows SEM micrographs of the Ni film before reaction and after 1 week of continuous operation. The surface area was determined by measuring the oxy-

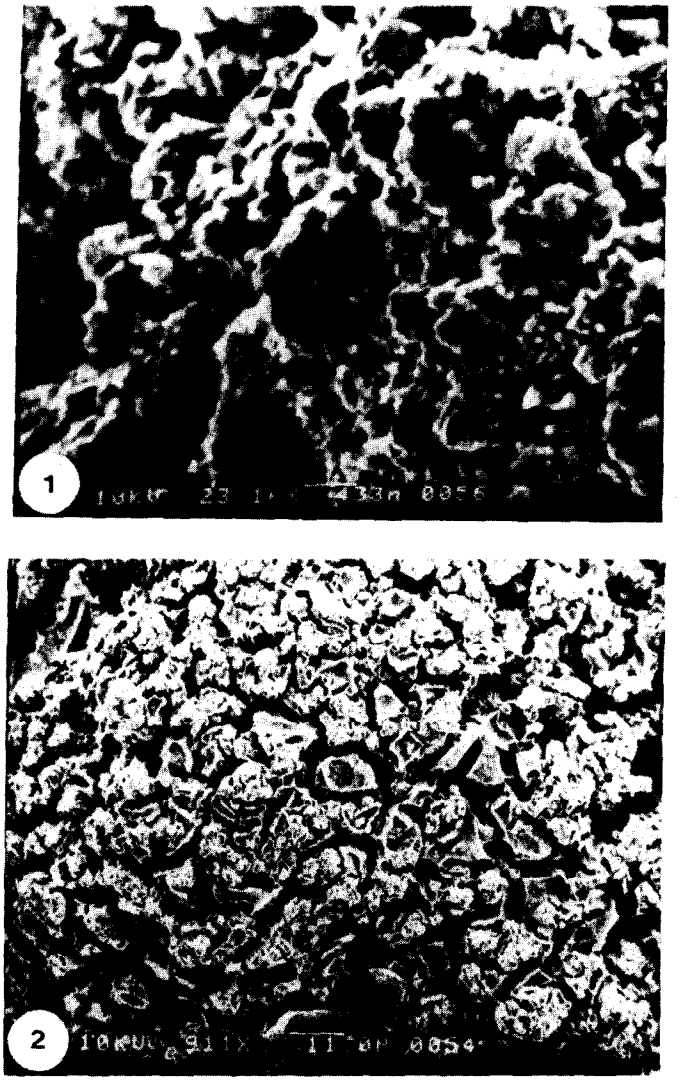

FIG. 2. Scanning electron micrograms: (1) and (2) before reaction; (3) and (4) after reaction.

gen uptake of the catalyst (moles O_2) as described in detail elsewhere (*25*). At 350°C a 250-mg amount of catalyst could adsorb approximately $(1.5 \pm 1) \times 10^{-6}$ mol of oxygen.

RESULTS

The reaction kinetics as well as the surface oxygen activity behavior were examined at temperatures 238–408°C and atmospheric total pressure. The oxygen partial pressure in the reactor was varied between 0 and 0.15 bar and that of hydrogen between 0 and 0.105 bar. Nitrogen was used as a diluent. Due to safety considerations the region of oxygen–hydrogen compositions employed was limited by the lower explosion limit of hydrogen in oxygen (*27*).

Three reactor cells were used in this study. The reactors differed only in the amount of catalyst used as shown in Table 1. The reaction rate was calculated from the appropriate mass balance for oxygen

$$r = 2Q(x^{\circ}_{O_2} - x_{O_2}), \qquad (6)$$

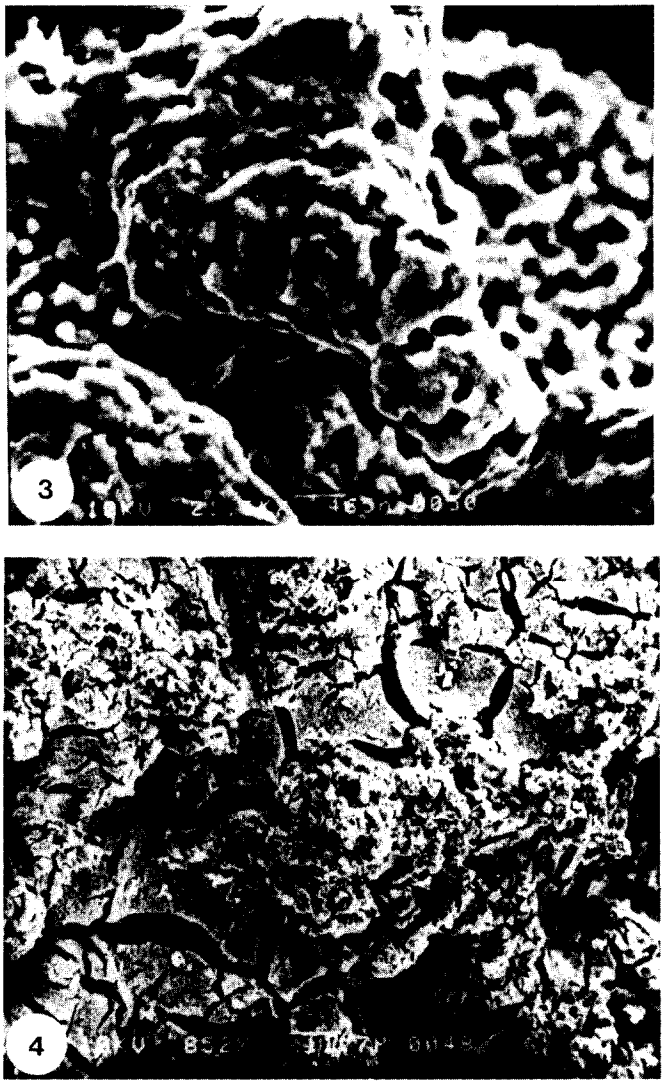

FIG. 2—*Continued.*

where Q is the total molar feed flow rate and $x^{\circ}_{O_2}$, x_{O_2} the mole fractions of oxygen in the feed and the outlet, respectively.

TABLE 1

Reactor cell no.	Catalyst load (mg)
R1	380
R2	340
R3	285

In order to verify absence of concentration differences between bulk fluid and catalyst surface the reaction rate was examined as a function of the feed flow rate. This was done using reactor R1 at the highest temperature employed in this study, i.e., 408°C. Since the rate dependence on P_{O_2} and P_{H_2} was unknown both partial pressures were kept constant inside the reactor by appropriate variation of the inlet gas composition.

It was concluded (*26*) that external mass

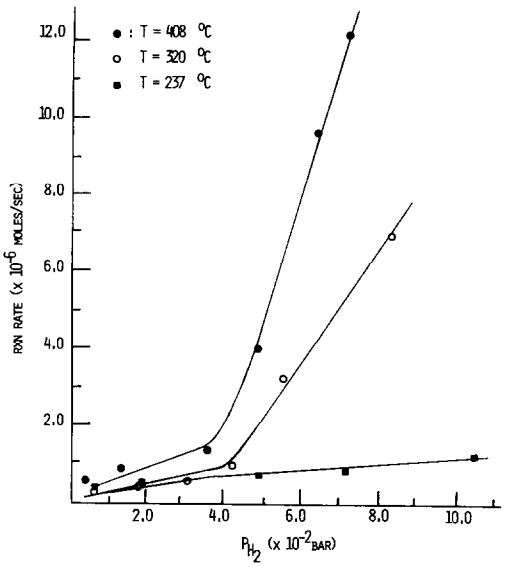

FIG. 3. Effect of P_{H_2} on reaction rate.

transfer is not significant at flow rates above 350 cm³/min. All the kinetic data shown below were taken with flow rates higher than 350 cm³/min. Intrapellet diffusion limitations were also unimportant. This was verified by using the Weisz–Prater criterion (*28*) and considering the nickel film as a porous slab. Using the experimental data the value of the generalized Thiele modulus calculated (*26*) was less than 0.008. Furthermore, the absence of intrapellet diffusion limitations was verified by changing the film thickness and not observing any change in the values of a_0 measured for the same gas composition (*25, 16*).

The possibility of homogeneous hydrogen oxidation was investigated by using a stabilized zirconia tube identical to those used as reactors but without depositing catalyst on its bottom. Oxygen and hydrogen passed through the "blank" reactor under conditions similar to those during our kinetic studies. The homogeneous gas-phase reaction rate thus measured was found to be essentially zero at temperatures lower than 320°C. Nevertheless at 350°C the homogeneous rate was about 1% of the catalytic reaction rate under the same conditions (*26*) and at 408°C it was up to 8% of the heterogeneous rate. The kinetic results shown below for 360 and 408°C have been corrected by subtracting the homogeneous effect.

Steady-State Kinetics

The dependence of a_0 and the reaction rate on P_{H_2} was studied at five different temperatures, holding the partial pressure of oxygen in the outlet approximately constant. Data were taken at 237, 280, 320, 360, and 408°C. Figure 3 contains some of these kinetic data, i.e., 408, 320, and 237°C. The reaction rate seems to be higher than first order with respect to P_{H_2} at the higher temperatures and the order seems to decrease with decreasing temperature. In Fig. 4 the corresponding values of the surface oxygen activity a_0 are plotted vs P_{H_2}.

Kinetic and potentiometric measurements for approximately constant P_{H_2} were taken at the above temperature. In Fig. 5 the reaction rate is plotted vs P_{O_2} while Fig. 6 shows the dependence of a_0 on P_{O_2}. It can be seen in Fig. 5 that the rate is initially negative order with respect to oxygen until it reaches a minimum value and then increases slightly with increasing P_{O_2}. That peculiar rate dependence is not observed at

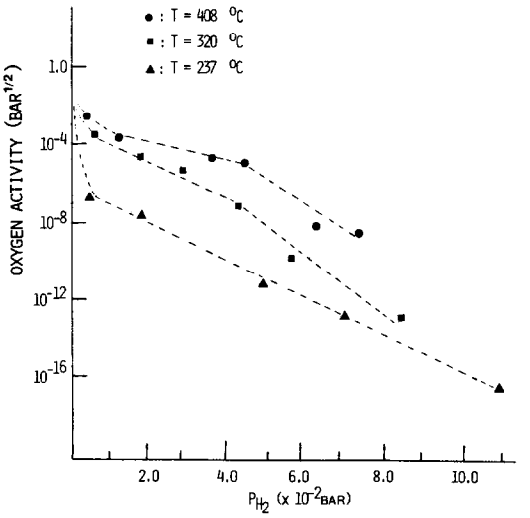

FIG. 4. Effect of P_{H_2} on surface oxygen activity a_0.

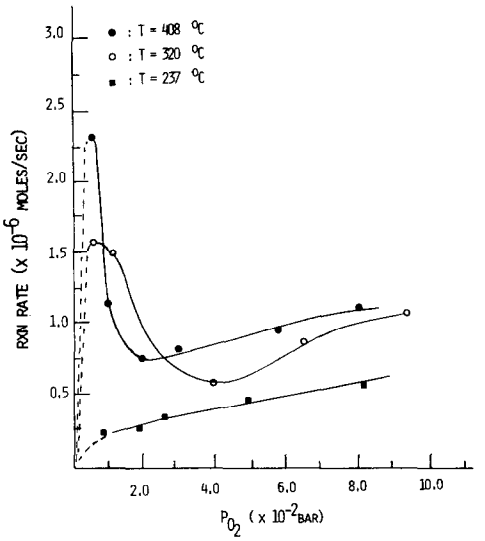

FIG. 5. Effect of P_{O_2} on reaction rate.

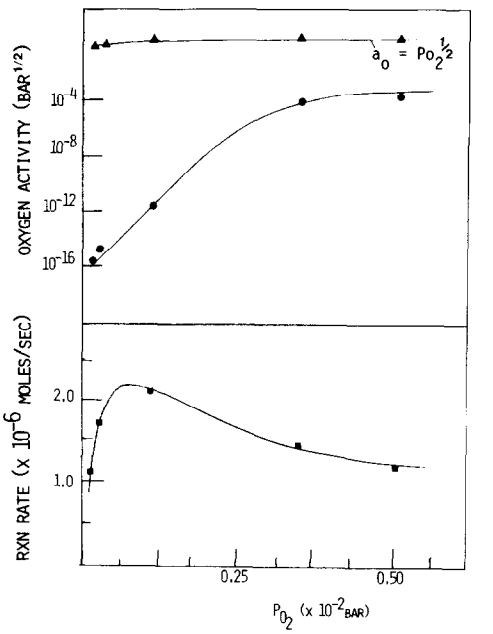

FIG. 7. Rate and a_0 dependence on P_{O_2}.

the lowest temperature examined, i.e., 237°C. The corresponding a_0 is shown in Fig. 6. In view of the rather unusual dependence of the reaction rate on P_{O_2} at low oxygen partial pressures, detailed measurements were undertaken to further elucidate this dependence in the region 0–0.01 bar P_{O_2} and 300–408°C. Kinetic and potentiometric results obtained with reactor R2 at 408°C are shown in Fig. 7. It can be seen that the reaction rate goes through a maximum at very low partial pressures of oxygen. The surface oxygen activity shown in the top part of Fig. 7 increases dramatically with increasing P_{O_2} until it reaches values of the order of 10^{-4} bar$^{1/2}$ and then it becomes very weakly dependent on P_{O_2}. The curve of triangles shown in the same figure corresponds to the value of a_0 calculated assuming thermodynamic equilibrium between gaseous and adsorbed oxygen. These equilibrium values are found by just measuring P_{O_2} in the bulk and using Eq. (5). Experimental curves similar to those shown in Fig. 7 were obtained at temperatures as low as 300°C.

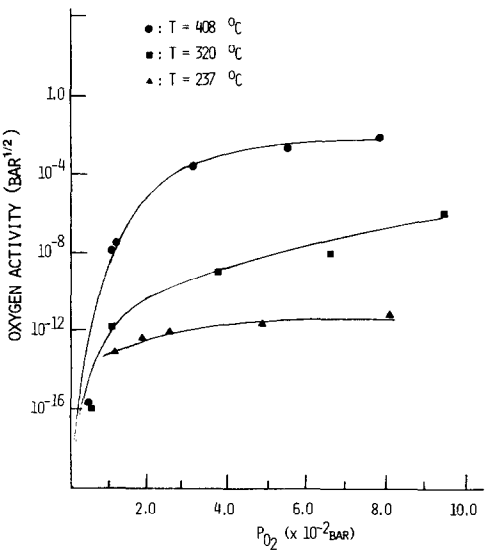

FIG. 6. Effect of P_{O_2} on oxygen activity.

It must be pointed out that the above-presented data represent stable steady states. Oscillatory phenomena were not observed under these conditions although the time required for the system to reach the final reported values was of the order of a few hours in most of the experiments. We considered that steady state was achieved when the voltage and the outlet oxygen

concentration readings did not change by more than 2% over a period of 2 h. It should be emphasized that the response time of the voltage readings was very distinctive. When only diluted hydrogen was introduced in the reactor the time required to get the final reading was of the order of seconds. The same was observed when only air was introduced in the reactor although the response time was a bit longer (1–5 min). In the case, however, where a reactive mixture of H_2 and air was introduced, the response was very slow and in most of the experiments the final steady states were reached after two or more hours.

Oscillatory States

Reactor R3 (Table 1) was used in this set of experiments. Before each experiment the reactor was left overnight in a hydrogen–nitrogen stream at 400°C. Thus reacting mixtures were introduced after the catalyst was exposed to a reducing environment. Signs of oscillatory behavior either in the voltage or the outlet O_2 concentration did not appear until about 30–40 min after the beginning of the experiment and became fully developed several hours later. Most of the oscillations observed were of the relaxation type, characterized by a sharp increase in the rate followed by a slow gradual decrease. The periods observed varied from 4 to 50 min and the amplitude ranged from 1 to 50%, defined as deviation from the average value. The period was defined as the time between two distinctive consecutive peaks and was not easy to determine unequivocally in some experiments. The surface oxygen activity measured with SEP oscillated as well and in general an increase in the reaction rate was accompanied by a decrease in a_0.

The effect of P_{O_2} on the period and amplitude of oscillations is shown in Fig. 8 for 408°C. A decrease in P_{O_2} corresponds to increase in reaction rate (Eq. (6)) and an increase in the emf corresponds to a decrease in a_0 (Eq. (4)). It was observed that the oscillatory region was bounded by a stable steady-state region and thus a minimum and a maximum P_{O_2} exists at which oscillations appear and disappear, respectively. The amplitude of the oscillations increases with increasing P_{O_2}, reaches a maximum at about 0.67×10^{-2} bar and then decreases, vanishing at $P_{O_2} \simeq 0.018$ bar. This is shown in Fig. 9.

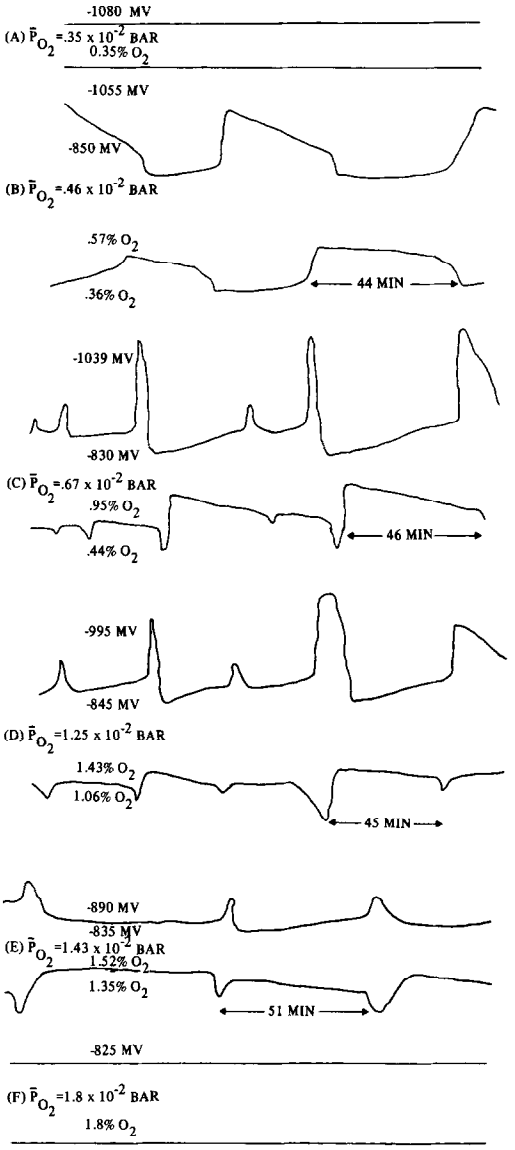

FIG. 8. Effect of P_{O_2} on rate and a_0 oscillations.

In the region where rate and emf oscillations were observed the surface temperature variation was very small (1–3°C). Only

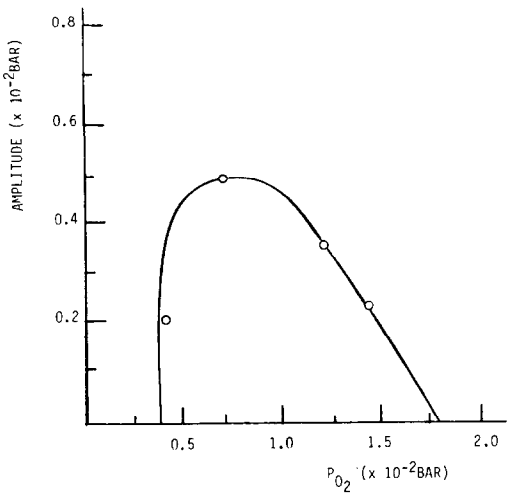

FIG. 9. Dependence of oxygen concentration amplitude of oscillations on P_{O_2} (T = 408°C, P_{H_2} = 0.087 bar).

in one experiment, at 408°C, were temperature variations as large as 12°C observed; in this experiment the amplitude of the reaction rate was 50%.

It is worth mentioning that the emf and P_{O_2} oscillations were not always observed simultaneously. In a few cases the voltage oscillated while P_{O_2} remained constant while in other cases the opposite phenomenon was observed as shown in Fig. 10. Nevertheless that was observed in exceptionally few cases while as a rule a decrease in a_0 corresponded to increase in reaction rate.

DISCUSSION

The stable steady-state results presented in the previous section provided the following information:

1. For constant P_{O_2} and temperature the rate increases slowly with increasing P_{H_2} until $P_{H_2}/P_{O_2} \simeq 1$. Above this ratio the rate dependence on P_{H_2} becomes more pronounced so that the apparent reaction order is higher than 1 with respect to hydrogen (Fig. 3).

2. For constant P_{H_2} and temperature the rate increases sharply with P_{O_2}, reaches a maximum and then decreases sharply and goes through a minimum. The local minimum at 408 and 320°C (Fig. 5) could be partly due to the fact that P_{H_2} at the exit could not be kept absolutely the same (0.017 bars) for all the data points but varied slightly (3–4% variation from 0.017 bar). For high P_{O_2} the rate becomes almost independent of the oxygen partial pressure (Figs. 5, 7). This behavior is not followed by the reaction rate at the lowest temperature examined, i.e., 237°C.

3. In the presence of O_2–H_2 mixtures above the catalyst 1–4 h are usually required to reach steady state.

4. The surface oxygen activity reaches extremely low values for large P_{H_2}/P_{O_2} and in that regime the values of a_0 can be 10 orders of magnitude lower than those predicted assuming thermodynamic equilibrium between gaseous and adsorbed oxygen (Figs. 6, 7).

This deviation from equilibrium is far more significant than that observed by Vayenas *et al.* during ethylene oxidation on Pt and propylene oxide oxidation on Ag where sustained oscillations were also observed (*17, 18, 23, 29*). This strong deviation can be attributed to both high competition of H_2 and O_2 for the same surface sites and slow rate of adsorption of oxygen as has already been suggested by Luss *et al.* (*11*).

Figure 3 might be interpreted as indicating one of the following: (a) That the reaction is second, or generally higher than first

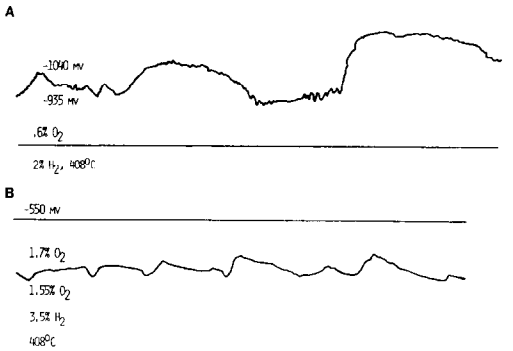

FIG. 10. (A) Voltage oscillates while O_2 outlet remains constant. (B) O_2 outlet oscillates while voltage remains constant.

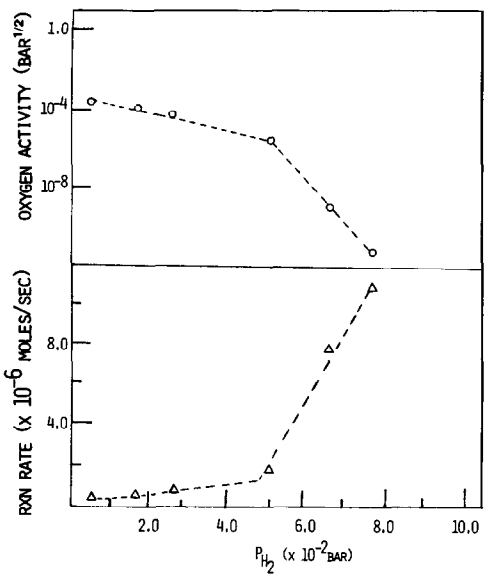

FIG. 11. Rate and a_0 dependence on P_{H_2}.

order with respect to P_{H_2}; this is highly unlikely for Langmuir–Hinshelwood kinetics; and (b) that more than one reaction producing H_2O occurs.

The latter interpretation is in harmony with Larson and Smith's observation that a stable oxide forms gradually on Ni surfaces, decreasing the activity of the catalyst (*4*). Peace and Taylor suggested that the oxidized material is essentially inactive as a catalyst (*30*). Quinn and Roberts (*31*) studied extensively the nature of the oxidized material formed and concluded that there are two types of oxide formed, stoichiometric NiO as well as a "dilute" Ni_mO ($m \simeq 3$). A similar interpretation can be given to the rate and oxygen activity dependence on P_{H_2} shown again in Fig. 11: for low P_{H_2} (or equivalently low P_{H_2}/P_{O_2}) the nickel oxide is dominant on the surface and because of its inactivity the reaction rate is very slow. At high values of P_{H_2}/P_{O_2} the oxide coverage is diminished by hydrogen and thus high reaction rates are obtained. Consequently the whole region examined can be divided into two, one of primarily reduced surface and one of primarily oxidized surface. We assume that Ni and its oxide may coexist under reaction conditions as Reikert (*32*) has previously shown. Using the data from the five temperatures examined one can calculate the apparent activation energies in the two regions as shown in Fig. 12. The values thus obtained are 2.8 and 11.6 kcal/mole on the oxidized and reduced surface, respectively.

The above hypothesis of reduced–oxidized behavior is also in agreement with the rate and a_0 dependence on P_{O_2} (Figs. 6, 7). For low P_{O_2} the surface is primarily clean and thus very active. In that region high reaction rates are obtained and the surface oxygen activity a_0 is extremely low because of (a) depletion of surface oxygen through reaction with hydrogen and (b) excess gaseous hydrogen competing with oxygen for the same catalyst sites. As P_{O_2} increases the oxide coverage starts to be significant and because of its inactivity the rate drops. For high values of P_{O_2} the rate of H_2O formation is the sum of rates of reaction of adsorbed oxygen with hydrogen and reduction of nickel oxide by hydrogen. At the lowest temperature (237°C) the surface remains primarily oxidized over the whole region of partial pressures of oxygen examined and thus neither maximum nor minimum on the reaction rate is observed (Fig. 5).

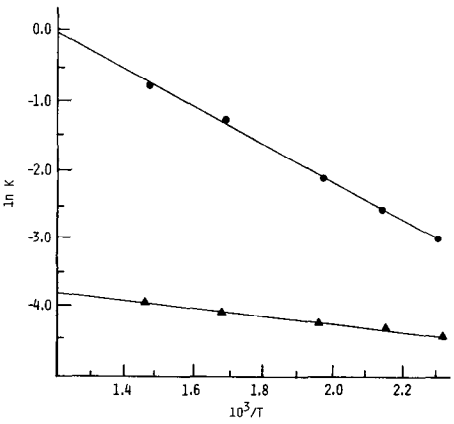

FIG. 12. Temperature dependence of apparent reaction rate constant on reduced (●) and oxidized (▲) surface.

In Fig. 7 one can notice a remarkable high deviation from thermodynamic equilibrium between surface and gaseous oxygen, especially at low P_{O_2}. This strong deviation decreases rapidly with increasing P_{O_2} and becomes almost independent of P_{O_2} for high P_{O_2}/P_{H_2} ratios. This observation further implies that SEP measurements reflect mainly the activity behavior of adsorbed atomic oxygen rather than any other type of oxygen accommodated on the metal surface as has been proposed in previous SEP studies as well (*16, 18, 15*).

Based upon the hypothesis of both chemisorption and oxidation of the nickel catalyst one can write the following equations for H_2 and O_2 interaction with the surface.

$$H_2 + 2m \rightleftharpoons 2\ m\text{–H} \qquad \text{(A)}$$

$$O_2 + 2m \rightleftharpoons 2\ m\text{–O} \qquad \text{(B)}$$

$$O_2 + 2m \rightleftharpoons 2\ m\text{–O}^* \qquad \text{(C)}$$

Here m stands for catalyst site and m–O* stands for nickel oxide species whereas m–O represents adsorbed atomic oxygen species.

The equilibrium constant for reaction (C) can be found from literature values (*33, 34*) and should be approximately equal to $K = 1/P_{O_2}^{1/2}$. Thus at 408°C the equilibrium constant is found to be $K = 8.2 \times 10^{13}$ which in turn gives a value of $P_{O_2} = 1.5 \times 10^{-28}$ and consequently $P_{O_2}^{1/2} = 1.2 \times 10^{-14}$. Based on the present results the formation of nickel oxide from gaseous O_2 seems to lack experimental support. This is because $P_{O_2}^{1/2}$ values measured are of the order of 10^{-2} even in the range of oxygen partial pressure where the maximum on the reaction rate is observed (Fig. 7, top curve).

An alternative model for adsorption and oxide formation would be

$$H_2 + 2m \rightleftharpoons 2\ m\text{–H} \qquad \text{(A)}$$

$$O_2 + 2m \rightleftharpoons 2\ m\text{–O} \qquad \text{(B)}$$

$$m\text{–O} + m \rightleftharpoons \text{m–O}^* + m \qquad \text{(C')}$$

The only difference between the two models is that in the second model the oxide forms from adsorbed oxygen as shown in step (C'). In this case the equilibrium constant will determine a minimum surface oxygen activity required for oxide formation $a_0^+ = 1/K$. At 408°C the value of a_0 thus calculated is $a_0^+ = 1.2 \times 10^{-14}$, i.e., very close to the values of a_0 obtained experimentally in the low P_{O_2} regime. As mentioned before, the relationship $a_0 <<< P_{O_2}^{1/2}$ is due to strong deviation from equilibrium between gaseous and adsorbed oxygen. If such an equilibrium were established both kinetic models would be equally incorrect.

Figure 13 shows the reaction rate as well as the a_0 behavior vs P_{O_2}. The horizontal dotted lines represent the values of $a_0^+ = 1/K$ for T = 408, 320, and 237°C. Note that at 237°C the a_0^+ line is well below the experimentally measured values of a_0. Indeed at that temperature no minimum or maximum reaction rate was observed within the range of P_{H_2}–P_{O_2} examined.

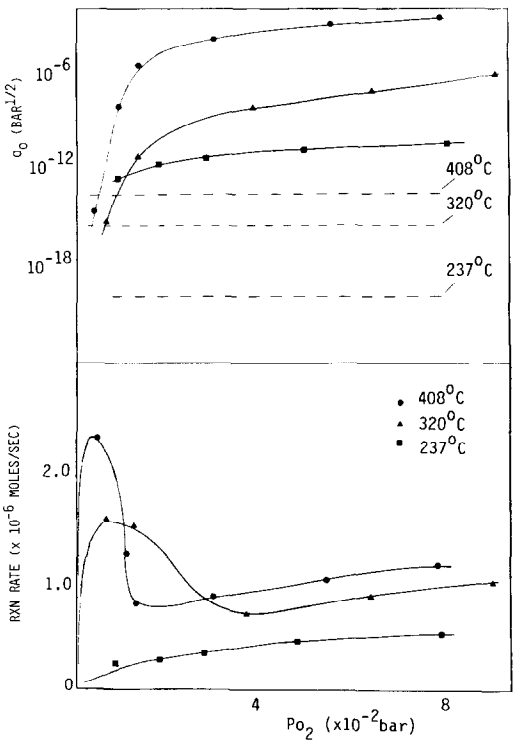

FIG. 13. Rate and oxygen activity dependence on P_{O_2} at 408, 320, and 237°C.

On the basis of the above observations the second model is much more successful in interpreting the kinetic and SEP results, but needless to say neither of the above models predicts oscillatory behavior without introducing any further assumptions. Vayenas *et al.* (*23*) proposed an oxidation–reduction dynamic model in order to explain the oscillations observed during ethylene oxidation on Pt. The above authors proposed that the surface platinum oxide forms only when a_0 exceeds the thermodynamic stability limit of surface platinum oxide. Kurtanjek *et al.*, although they did not propose a specific model, suggested that the oscillatory and chaotic phenomena observed during H_2 oxidation on Ni are most probably due to periodic oxidation–reduction of the surface. Sault and Masel used surface spectroscopic techniques to study the effect of surface protrusions on the oscillatory behavior of the reaction and concluded that oscillations are seen when the surface is covered by protrusions of 5–20 μm. As seen in Fig. 2, the nickel films used in the present study were quite rough both before and after completion of the experiments. An attempt to prepare a flat nickel film on the scale of micrometers over the stabilized zirconia surface would eliminate the catalyst–electrolyte–air interline the presence of which is absolutely necessary in obtaining successful SEP measurements (*15, 25*).

Before any attempt is made to explain the periodic phenomena observed during H_2 oxidation on Ni it would be most helpful to investigate more thoroughly and with the aid of SEP the parameters affecting the amplitude and shape of the oscillations as well as the boundaries within which periodic phenomena occur. The effect of P_{O_2} on the amplitude although very similar to that observed by Belyaev *et al.* (*7*) was studied at 408°C only and with one fixed value of P_{H_2} (Fig. 8). The technique of SEP could also be useful in the investigation of the previously reported hysteresis phenomena as well as the effect of different diluent gases on the oscillatory behavior of the reaction rate. A systematic study of the effect of T, P_{H_2}, and possibly feed flow rate on the rate and emf oscillations would provide additional valuable information that could be used in order to eliminate a number of candidate kinetic models. Experimental work toward that goal is already (*35*) in progress.

REFERENCES

1. Bond, G. C., "Catalysis by Metals." Academic Press, New York, 1962.
2. Sheintuch, M., and Schmitz, R. A., *Catal. Rev.-Sci. Eng.* **15**(1), 107 (1977).
3. Slinko, M. M., and Slinko, M. G., *Kinet. Katal.* **23**(6), 1421 (1982).
4. Larson, A. T., and Smith, F. E., *J. Amer. Chem. Soc.* **47,** 346 (1925).
5. Gidaspow, D., and Ellington, R. T., *AIChE J.* **10,** 714 (1964).
6. Mamedov, E. A., Popouskii, V. V., and Boreskov, G. K., *Kinet. Katal.* **14**(2), 523 (1973).
7. Belyaev, V. D., Slinko, M. M., Slinko, M. G., and Timoshenko, V. I., *Dokl. Acad. Nauk. SSSR* **324** (5), 1098 (1974).
8. Belyaev, V. D., *et al. Kinet. Katal.* **14,** 810 (1973).
9. Belyaev, V. D., Slinko, M. M., and Timoshenko, V. I., *Kinet. Katal.* **16,** 555 (1975).
10. Schmitz, R. A., Renola, G. T., and Garrigan, P. C., *Ann. N.Y. Acad. Sci.* **316,** 638 (1979).
11. Kurtanjek, Z., Sheintuch, M., and Luss, D., *J. Catal.* **66,** 11 (1980).
12. Kurtanjek, Z., Sheintuch, M., and Luss, D., *Ber. Bunsenges. Phys. Chem.* **84,** 374 (1980).
13. Sault, A. G., and Masel, R. I., *J. Catal.* **73,** 294 (1982).
14. Kurtanjek, Z., *Croat. Chem. Acta* **56**(1), 17 (1983).
15. Wagner, C., "Advances in Catalysis," Vol. 21, p. 323. Academic Press, New York, 1970.
16. Stoukides, M., and Vayenas, C. G., *J. Catal.* **69,** 18 (1981).
17. Vayenas, C. G., Lee, B., and Michaels, J., *J. Catal.* **66,** 36 (1980).
18. Stoukides, M., and Vayenas, C. G., *J. Catal.* **74,** 266 (1982).
19. Eigenberger, G., *Chem. Eng. Sci.* **33,** 1963 (1978).
20. Pikios, C. A., and Luss, D., *Chem. Eng. Sci.* **32,** 191 (1977).
21. Slinko, M. G., and Slinko, M. M., *Catal. Rev.-Sci. Eng.* **17,** 119 (1978).
22. Jensen, K., and Ray, W. H., *Chem. Eng. Sci.* **35,** 2439 (1980).
23. Vayenas, C. G., Georgakis, C., Michaels, J., and Tormo, J., *J. Catal.* **67,** 348 (1981).
24. Sheintuch, M., and Schmitz, R. A., *ACS Symp. Ser.* **65,** 487 (1978).

25. Stoukides, M., and Vayenas, C. G., *J. Catal.* **64,** 18 (1980).
26. Saranteas, C., M.S. thesis, Tufts University, Mass., 1984.
27. Kirk-Othmer, "Encyclopedia of Chemical Technology," Vol. 12, p. 946, 3rd ed. Wiley, New York, 1978.
28. Froment, G. F., and Bischoff, K. B., "Chemical Reactor Analysis and Design." Wiley, New York, 1976.
29. Stoukides, M., Seimanides, S., and Vayenas, C. G., *ACS Symp. Ser.* **196,** 195 (1982).
30. Pease, R. N., and Taylor, H. S., *J. Amer. Chem. Soc.* **44,** 1637 (1922).
31. Quinn, C. M., and Roberts, M. W., *Trans. Faraday Soc.* **60,** 899 (1964); **61,** 1776 (1965).
32. Reikert, L., *Ber. Bunsenges. Phys. Chem.* **85,** 297 (1981).
33. Perry-Chilton, "Chemical Engineering Handbook," 5th ed. McGraw–Hill, New York, 1973.
34. Vasil'eva, I. A., Sukhushina, I. S., Granousskaya, Zh. V., Balabaeua, R. F., and Maioroua, A. F., *Zh. Fiz. Khim.* **49,** 2169 (1975).
35. Saranteas, C., and Stoukides, M., in preparation.